JGR Biogeosciences

RESEARCH ARTICLE
10.1029/2024JG008297

Distinguishing the Impacts and Gradient Effects of Climate Change and Human Activities on Vegetation Cover in the Weihe River Basin, China

Wen-Bo Lv[1], Fang-Mei Liu[1], Kai Cai[1], Yue Cao[1], Meng-Ling Deng[1], Wei Liang[1], Jian-Wu Yan[1], and Guang-Yu Wang[2]

[1]School of Geography and Tourism, Shaanxi Normal University, Xi'an, China, [2]National Park Research Centre, Faculty of Forestry, University of British Columbia, Vancouver, BC, Canada

Key Points:

- Single factor's effect intensity and direction on vegetation cover change changed under the interaction with others
- The impact of extreme climatic conditions on the dynamics of vegetation coverage should not be overlooked
- The intensity and direction of the impact of factors varied in diverse vegetation gradients

Correspondence to:
J.-W. Yan and G.-Y. Wang,
yanjw@snnu.edu.cn;
guangyu.wang@ubc.ca

Citation:
Lv, W.-B., Liu, F.-M., Cai, K., Cao, Y., Deng, M.-L., Liang, W., et al. (2024). Distinguishing the impacts and gradient effects of climate change and human activities on vegetation cover in the Weihe River Basin, China. *Journal of Geophysical Research: Biogeosciences*, *129*, e2024JG008297. https://doi.org/10.1029/2024JG008297

Received 11 JUN 2024
Accepted 1 OCT 2024

Author Contributions:
Conceptualization: Wen-Bo Lv
Data curation: Wen-Bo Lv, Yue Cao
Methodology: Wen-Bo Lv, Yue Cao, Wei Liang
Project administration: Fang-Mei Liu, Wei Liang
Resources: Meng-Ling Deng
Software: Kai Cai
Supervision: Jian-Wu Yan
Visualization: Wen-Bo Lv, Kai Cai
Writing – original draft: Fang-Mei Liu, Meng-Ling Deng
Writing – review & editing: Jian-Wu Yan, Guang-Yu Wang

Abstract Vegetation cover is crucial for ecosystem stability, responding sensitively to climate change and human activities, and is prone to irreversible degradation. However, the mechanisms driving vegetation variations due to natural and anthropogenic factors still need to be fully understood. This study focused on the Weihe River Basin to elucidate the response mechanism of vegetation cover change to climate change and human activities from 2001 to 2020. Long time-series multi-source data were combined with a pixel dichotomy model, Theil–Sen median trend analysis, and Mann-Kendall test to examine the trends and delineate five gradients in vegetation cover change. Additionally, Extreme Gradient Boosting, the Shapley value, and a structural equation model were employed to investigate the multidimensional response of vegetation cover in the basin as a whole and different vegetation cover gradients. The results revealed a general upward trend in vegetation coverage in the Weihe River Basin from 2001 to 2020. Topographic conditions and human activities were identified as primary influencers. Notably, accounting for climate change, particularly about changes in maximum climatic variables, was found to be essential, with temperature changes exerting a greater impact on vegetation cover variations compared to precipitation changes. The interaction between human activities, climate change, and topographic conditions can alter the intensity of each factor's effect. The direction of indicators mentioned above varied across the vegetation cover gradients, emphasizing the need for localized strategies to improve vegetation. These findings offer valuable insights into ecological protection and vegetation restoration in the Weihe River Basin.

Plain Language Summary Understanding how vegetation cover responds to climate change and human influence is vital for maintaining ecosystem health. This study focused on the Weihe River Basin, a region prone to ecological fragility, to explore how vegetation cover responds to human activity and climate change factors, considering basic topographical factors. Models that can identify trends, rank contributions, explore interactions between variables, and quantify the direct and indirect effects of variables were utilized. By analyzing various data and using different models, we found that vegetation coverage generally increased over this period. Factors such as topography and human activities greatly influenced vegetation cover change. Surprisingly, temperature fluctuations had a more substantial impact on vegetation cover than changes in precipitation. Moreover, the interaction between human activities, climate change, and topography can change the intensity and direction of the factor's effect on vegetation cover change. The effects varied across areas with different vegetation cover change conditions of the basin. These findings provide valuable insights for guiding ecological protection and vegetation restoration efforts in the Weihe River Basin.

1. Introduction

Significant changes in terrestrial ecosystems have been observed in recent decades due to the escalating effects of global climate change and human activities (Piao et al., 2019). Vegetation, as a crucial component of terrestrial ecosystems, serves as a connective link between the atmosphere, water bodies, and soil (Fang et al., 2020; Zhou et al., 2014), playing a vital role in regulating regional climate, maintaining surface energy balance, and preserving biodiversity (Piao & Fang, 2001; Piao et al., 2001). Therefore, investigating the characteristics and trends of vegetation cover changes, as well as revealing the influencing factors of vegetation dynamics and gradient effects, has emerged as a central focus of current research on global change.

Numerous studies emphasize that vegetation cover changes are primarily influenced by climate change and human activities (Ebrahimi Khusfi & Zarei, 2020; Naeem et al., 2020). The identification and quantification of the effects of these factors on vegetation coverage have been central to much research (Shi et al., 2021; C. Zhang et al., 2013). In recent years, China's notable contribution to the substantial increase in vegetation change in the north temperate zone has attracted attention to its specific vegetation characteristics (Piao et al., 2020). The correlation between vegetation coverage and temperature in China is negative, while that with precipitation is positive and the effect of precipitation on vegetation cover surpasses that of temperature (Lin et al., 2022; L. Zhu et al., 2023). However, variations in study outcomes are evident due to diverse regions and methodologies, reflecting the complexity of vegetation traits and their influential factors (M. Jiang et al., 2021; Ma et al., 2021; Qu et al., 2018).

Previous research has primarily examined the role of natural factors as drivers of vegetation cover. Correlation analysis has been conducted to investigate the relationship between temperature, precipitation, and vegetation cover (C. Chen et al., 2019). Convergent cross-mapping is also utilized to depict the relationship between temperature, precipitation, evapotranspiration, and vegetation coverage (Wu et al., 2023; J. Zhang et al., 2018; Y. Zhang et al., 2018). The impact of climatic factors, surface temperature, soil moisture, and precipitation on vegetation cover has been investigated via Granger causality testing (V. Kumar et al., 2023). In addition, factors such as aspect, soil type, and landform type have been considered to analyze the response mechanism of vegetation cover change (C. Zhu et al., 2019). The effects of human activities on regional vegetation cover are more intricate and multifaceted as they are closely tied to vegetation resources. Recent studies indicate that ecological reforestation, pasture restoration projects, and grazing ban policies tend to exert favorable effects on vegetation coverage while practices such as indiscriminate logging, hill fires, urban expansion, and mineral extraction can disrupt the growth space of vegetation coverage, ultimately leading to degradation (Feng et al., 2020; A. Kumar et al., 2017; Remy et al., 2017).

The aforementioned research underscores the dynamic change in vegetation coverage resulting from the interplay of multiple driving forces. It is crucial to quantitatively analyze the degree of the contribution and interactive effects of various influencing factors to effectively monitor regional vegetation cover and protect ecosystems. Previous studies typically treated climatic and anthropogenic factors as independent variables, utilizing statistical methods such as linear regression (W. Zhao et al., 2019), geographically weighted regression (X. Zhang et al., 2017), partial least squares regression (C. Deng et al., 2018), correlation analysis (C. Chen et al., 2019), and residual analysis (L. Jiang et al., 2017) to explore the relationship between vegetation cover changes, climate factors, and human activities. However, the effects of the intricate interplay between natural and anthropogenic factors on vegetation changes are rarely explored. While GeoDetector can measure the impact of influencing factors on vegetation change, including individual natural factors and the interactions between two factors (Huo & Sun, 2021), it is limited to detecting the interaction involving only two factors. In fact, vegetation cover change is driven by a system of multiple factors and their interactions. Although there are statistical techniques for measuring the interaction between two variables, several models, such as correlation analyses, are unable to accurately gauge the influence of a single variable by removing the impacts of other variables, hence resulting in biased outcomes. Moreover, existing research rarely distinguishes areas with different vegetation cover gradients, resulting in their conclusions and solutions that may lack local adaptation.

In summary, by adopting the Weihe River Basin, located in the east of the northwest inland of China, as a case study, this study took fraction of vegetation cover as the characterization index, integrated long-term multi-source data with topological, climate change, and anthropogenic factors to comprehensively evaluate the impact of climate change and land use changes on vegetation cover change from 2001 to 2020. In particular, we employed interpretable machine learning and Structural Equation Models to explore the temporal and spatial evolution characteristics of vegetation cover and its multi-dimensional response to climate change and human activities in the Weihe River Basin as a whole and on five vegetation gradients. This contributes to existing research and provides detailed suggestions for the continuous improvement of vegetation coverage in the basin.

2. Materials and Methods

2.1. Study Area

As the first major tributary of the Yellow River, the Weihe River is located in the east of the northwest inland of China. It flows through Gansu, Ningxia, and Shaanxi provinces, with a total length of 818 km. The basin has a

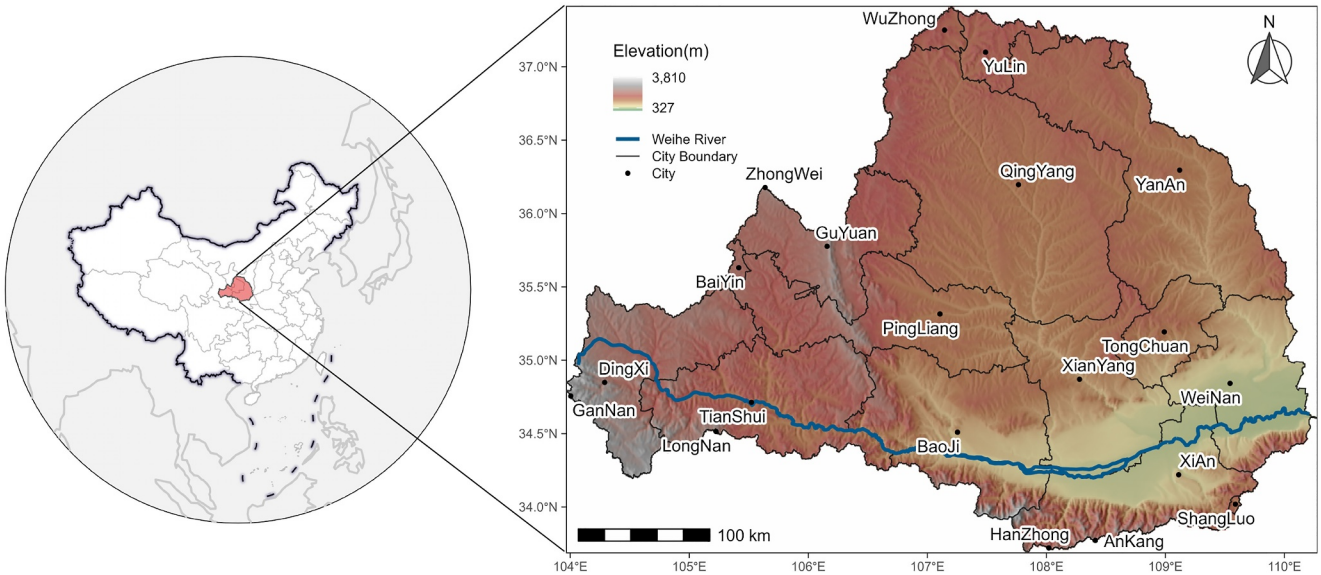

Figure 1. Location of Weihe River Basin and distributions of elevation.

drainage area of 13.48×10^5 km^2, located within 33.5°–37.5°N in latitude and 103.5°–110.5°E in longitude. The Weihe River Basin exhibits a gradual decrease in elevation from northwest to southeast, ranging from 327 to 3,841 m. To the north lies the Loess Plateau, while to the south stretches the Qinling Mountains. The average annual precipitation and average annual temperature of the basin range from 600 to 800 mm and 7.8–13.5°C, respectively (C. Zhang et al., 2021). The Weihe River Basin is situated in a transitional zone between arid, continental monsoon climates, and humid areas, experiencing the combined effects of monsoon and westerly circulation. The ecological environment in the basin is fragile and sensitive to climate change, which impacts both ecological protection and high-quality development in the middle and lower reaches of the Yellow River. Therefore, it is crucial to enhance ecological protection and management in the Weihe River Basin (Nie et al., 2024). The study area's location and administrative divisions are illustrated in Figure 1.

2.2. Data

2.2.1. Data Sources

The selected variables and their data sources used in this study are presented in Table 1. The temperature and precipitation data sets consist of monthly average temperature and monthly precipitation data spanning from 1901 to 2023, with a spatial resolution of 1 km (Ding & Peng, 2020; Peng et al., 2019). We picked up data from 2001 to 2020 among them, and these data were obtained from the National Tibetan Plateau Scientific Data Center. The enhanced vegetation index (EVI, which was employed to calculate the fraction of vegetation cover change (FVCC), Vermote & Wolfe, 2015), digital elevation model (DEM), and land use (Lu) data sets were derived from the Moderate Resolution Imaging Spectroradiometer (MODIS) Terra Daily EVI data set, NASA Shuttle Radar Topography Mission (SRTM) Digital Elevation 30 m data set (Farr et al., 2007), and MCD12Q1.061 MODIS Land Cover Type Yearly Global 500 m data set (Friedl & Sulla-Menashe, 2022), respectively, all of which were accessed through the Google Earth Engine platform. The land use data were specifically selected for the years 2001 and 2020, while the elevation data, treated as a constant over the long term, were acquired for the year 2000. Other data sources were confined to the period between 2001 and 2020. The population (Pd) and nighttime light data (Ntl) were collected from the WorldPop website and the China Long Time-Series Nighttime Light Dataset (WorldPop & Bondarenko, 2020; Zhong et al., 2022), respectively, spanning from 2001 to 2020.

2.2.2. Data Processing

In order to encapsulate the changes in climate patterns and vegetation coverage, we employ a uniform approach of utilizing change variables within our analytical modeling framework. The variables selected for this study include FVCC to represent changes in vegetation coverage, and topographic variables such as elevation (Elev), slope

Table 1
Selection of Driving and Representing Factors for Vegetation Cover Change

Type	Factor name	Time range	Data source	Data chaining
Topographical factor data	Elev	2000	NASA SRTM Digital Elevation 30 m data set for the GEE platform	https://developers.google.com/earth-engine/datasets/catalog/USGS_SRTMGL1_003#bands
	Slope	2000		
	Aspect	2000		
Climatic data	TmpAvgC	2001–2020	1-km monthly mean temperature data set for China (1901–2023) for the National Tibetan Plateau/Third Pole Environment Data Center	https://cstr.cn/18406.11.Meteoro.tpdc.270961, https://doi.org/10.11888/Meteoro.tpdc.270961
	TmpMaxC	2001–2020		
	TmpMinC	2001–2020		
	PreSumC	2001–2020	1-km monthly precipitation data set for China (1901–2023) for the National Tibetan Plateau/Third Pole Environment Data Center	https://doi.org/10.5281/zenodo.3114194
	PreMaxC	2001–2020		
	PreMinC	2001–2020		
Human activity data	PdC	2001–2020	WorldPop website	https://hub.worldpop.org/doi/10.5258/SOTON/WP00675
	NtlC	2001–2020	China Long Time Series Night Light Dataset (2000–2020)	https://doi.org/10.3974/geodb.2022.06.01.V1.
	LuC	2001,2021	The MCD12Q1.061 MODIS Land Cover Type Yearly Global 500 m data set for the GEE platform	https://developers.google.com/earth-engine/datasets/catalog/MODIS_061_MCD12Q1#bands
Vegetation cover change	FVCC	2001–2020	MODIS Terra Daily EVI data set for the GEE platform	https://developers.google.com/earth-engine/datasets/catalog/MODIS_MOD09GA_006_EVI#bands

(Slope), and aspect (Aspect). Climate change is represented through variables such as the annual average temperature change (TmpAvgC), annual monthly maximum temperature change (TmpMaxC), annual monthly minimum temperature change (TmpMinC), annual total precipitation change (PreSumC), annual monthly maximum precipitation change (PreMaxC), and annual monthly minimum precipitation change (PreMinC). Human activities are characterized by variables such as population density change (PdC), nighttime light brightness change (NtlC), and land use change (LuC).

Elevation data were processed using the Google Earth Engine platform to calculate slope and aspect data, and the aspect classification was redefined according to sunny, semi-sunny, shady, and semi-shady slope categories.

For the temperature and precipitation data, we took their extreme effects on the ecosystem structure, function, and stability into consideration. The maximum and minimum values of precipitation within a year were extracted and used as the monthly maximum and monthly minimum precipitation values of that year. The maximum and minimum temperature data were calculated in the same way. Annual total precipitation was obtained by summing precipitation data for all months of the year. In contrast, the average annual temperature was calculated by averaging the mean temperature (notice that mean temperature is what it is in the data set) of all the months of the year.

The maximum value of daily EVI data was identified as the monthly maximum value. We then averaged the monthly maximum values of each year to get an annual EVI value, and the fraction of vegetation cover (FVC) was calculated using a pixel dichotomy.

After unifying the nighttime light data to the WGS84 coordinate system, elevation data were used as a template to standardize the resolution to the smallest row and column dimensions (557 rows * 891 columns). The land use data were unified using nearest neighbor interpolation, while other data were unified using linear interpolation.

The numerical variables were time-dependent multiple linear regression. The slopes were calculated to characterize the temporal changes of variables such as annual average temperature, annual monthly maximum temperature, annual monthly minimum temperature, annual total precipitation, annual monthly maximum precipitation, annual monthly minimum precipitation, population density, nighttime light brightness, and FVC. These slopes were obtained as variables: TmpAvgC, TmpMaxC, TmpMinC, PreSumC, PreMaxC, PreMinC, PdC, NtlC, and FVCC.

Categorical variables (e.g., aspect and land use type) were converted into numerical variables as input to models using one-hot encoding. The one-hot encoding is an approach that represents each category as a vector of 0 and 1s, with a 1 in the position corresponding to the category and 0s elsewhere. Meanwhile, we used changes of land use type grid pixels between 2001 and 2020 to create new categories of land use type change instead of using land use categories for each individual year. These variables, among other climatic factors and human activity factors calculated above, were utilized to pre-train a random forest model. The feature importance values of the random forest model were obtained through ten-fold cross-validation and normalized to the range of 0–1, resulting in numerical variables for aspect and land use change.

Numerous 1,500 × 1,500 m grids were then established within the study area, with the centers of the corresponding grid points designated as sample points. If the sample point has one null value variable, whether it's an independent variable or a dependent variable, the sample point will be dropped. Finally, we got 59949 sample points.

2.3. Methodology

This study initially employed the pixel dichotomy method to calculate the vegetation coverage of the Weihe River Basin based on EVI data. Following this, numerous 1,500 × 1,500 m grids were established within the study area, with the centers of the corresponding grid points designated as sample points. The raster data processed in Section 2.2 was sorted into spatial vector point data format via point extraction. An interpretable machine-learning model for the global Weihe River Basin was subsequently developed using the processed sample points. Finally, based on the five-category zoning of vegetation change trends obtained from the Sen-MK trend test, 120 sample points were collected from each zone as samples for various vegetation change trends within the basin using spatial equalization sampling methods. Structural Equation Modeling was then constructed to further attribute the vegetation cover change of the Weihe River Basin to the vegetation cover change gradients. The overall technical roadmap of this study is presented in Figure 2, and the principal research methods are outlined below.

2.3.1. Calculating the Fraction of Vegetation Cover (FVC) With a Pixel Dichotomy

FVC refers to the percentage of the vertical projection area of vegetation (including leaves, stems, and branches) on the ground as a proportion of the total area of the statistical zone. It can effectively reflect information such as the growth status and biomass of vegetation. The FVC data is derived from the Enhanced Vegetation Index (EVI) data using the pixel dichotomy method, a vegetation cover estimation model in which pixels are divided into pure and non-pure pixels. In general, pure pixels typically represent areas with a single land cover type, while mixed pixels encompass multiple land cover types (Xie, 2021). FVC is calculated as follows:

$$\mathrm{FVC} = \frac{\mathrm{EVI} - \mathrm{EVI}_{\mathrm{soil}}}{\mathrm{EVI}_{\mathrm{veg}} - \mathrm{EVI}_{\mathrm{soil}}},$$

where $\mathrm{EVI}_{\mathrm{soil}}$ represents the EVI value of pure soil cover pixels; and $\mathrm{EVI}_{\mathrm{veg}}$ represents the EVI value of pure vegetation cover pixels (X. Zhang et al., 2017).

A 5% confidence interval is used to cut off the upper and lower values of EVI, that is, $\mathrm{EVI}_{\mathrm{veg}}$ is 95% of EVI, and $\mathrm{EVI}_{\mathrm{soil}}$ is 5% of EVI. The higher the FVC value, the higher the degree of vegetation coverage.

2.3.2. Theil-Sen Median Trend Analysis and Mann-Kendall Test

Theil-Sen median trend analysis, also known as Sen slope estimation, is a robust nonparametric statistical method used for trend analysis, particularly for long-time series data. Based on median estimation, this method is less

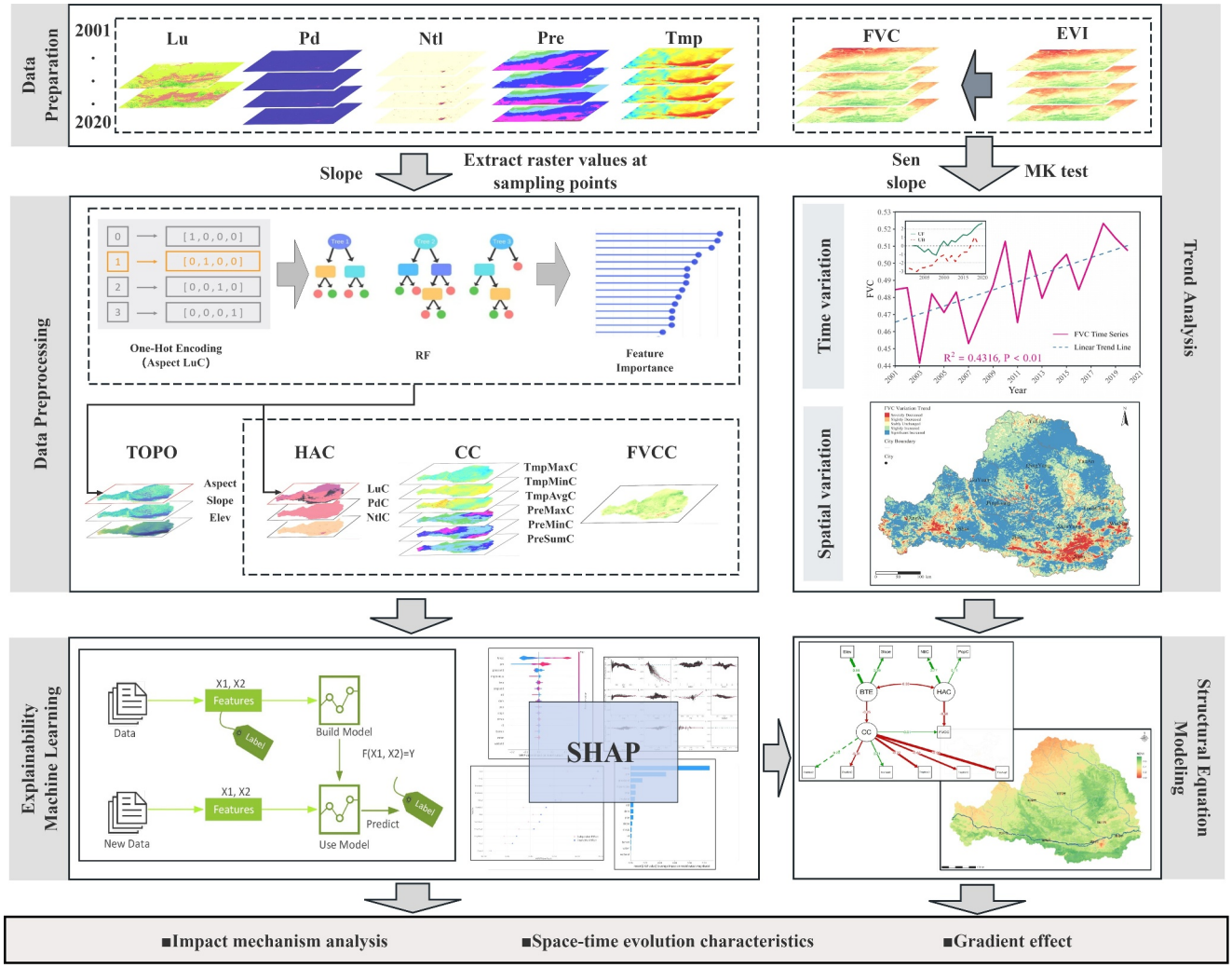

Figure 2. Overall technical roadmap employed in this study.

susceptible to measurement errors and outlier data, ensuring high computational efficiency (Nan et al., 2021; Yuan et al., 2013). We combined the Sen slope estimation with Mann-Kendall test to calculate trend values. The Theil-Sen median trend computes the median of the slopes across n(n − 1)/2 data combinations as follows:

$$S_{EVI} = \text{Median}\left(\frac{EVI_j - EVI_i}{j - i}\right),\ 2001 \le i < j \le 2020,$$

where $S_{EVI} > 0$ indicates an increasing trend in EVI, while $S_{EVI} < 0$ suggests a decreasing trend.

Mann-Kendall is a non-parametric statistical test method (Mann, 1945) employed to assess the significance of trends. Unlike methods relying on specific sample distributions, Mann-Kendall is not influenced by a few outliers (Kendall, 1949). It has proven to be effective for analyzing trend changes in the time series of precipitation, runoff, temperature, and water quality, among other elements (J. Cao et al., 2008), and is calculated as follows:

$$\{EVI_i\}, i = 2001, 2001, \ldots, 2020,$$

$$Z = \begin{cases} \dfrac{S-1}{\sqrt{s(S)}}, & S > 0 \\ 0, & S = 0, \\ \dfrac{S+1}{\sqrt{s(S)}}, & S < 0 \end{cases}$$

$$S = \sum_{j=i}^{n=1} \sum_{i=j+1}^{n} \mathrm{sgn}(EVI_j - EVI_i),$$

$$\mathrm{sgn}(EVI_j - EVI_i) = \begin{cases} 1, EVI_j - EVI_i > 0 \\ 0, EVI_j - EVI_i = 0 \\ -1, EVI_j - EVI_i < 0 \end{cases},$$

$$s(S) = \frac{n(n-1)(2n+5)}{18},$$

where EVI_i and EVI_j represent the EVI values of pixels in years i and j, respectively; n represents the length of the time series; and sgn is the sign function. The Mann-Kendall test Z statistic ranges within $(-\infty, +\infty)$. Under a given significance level α, $|Z| > u_{1-\alpha/2}$ indicates significant changes in the study series at the α level.

Sequential Mann-Kendall (seqMK) is an extension of the Mann-Kendall trend test, estimating the breakpoint when the trend occurs. seqMK trend test is usually used to identify abrupt changes in time series by using both a progressive and a regressive series across each other. We can calculate U value from the following formula:

$$U = \frac{S_i - E(S_t)}{\sqrt{Var(S_t)}}$$

where $E(S_t)$ and $Var(S_t)$ are Expectation and Variance of S value.

UF is calculated in a progressive series (1,2, … t, …n), and UB is calculated in a reversed one (n, n−1, …, 1).

2.3.3. XGBoost and Shapley Value

Gradient boosting is an ensemble learning algorithm that optimizes the objective function by iteratively shrinking the residual through addition models (i.e., a weighted sum of several base models) (Friedman, 2001). Extreme Gradient Boosting (XGBoost), a variant of the gradient boosting algorithm (T. Chen et al., 2015), is a machine learning algorithm based on decision tree ensembles. XGBoost employs custom loss functions adaptable to various problems (e.g., classification and regression problems), exhibiting computability efficiency in differentiating the objective function and thereby accelerating model training. In addition, it incorporates a sparsity-aware algorithm to effectively handle sparse data. Through the introduction of L1 and L2 regularization terms into the objective function, XGBoost mitigates model complexity, avoiding overfitting. Moreover, its adoption of a column-block design facilitates parallel computation, augmenting overall computational efficiency.

The Shapley value is employed to quantify the contribution of each participant in a cooperative game to the game's overall payoff (Shapley, 1953). Widely utilized in the field of machine learning for assessing and interpreting feature importance, it operates within the framework of a cooperative game where each participant represents a feature, and the game's payoff represents the model's prediction result. In the cooperative game context, the Shapley value is computed by cumulating the contribution of all subsets of participants to the game payoff, representing the expected marginal contribution of the feature across different feature sets. The Shapley value for feature X_j in the model is expressed as follows:

$$\mathrm{Shapley}(X_j) = \sum_{S \subseteq N \setminus \{j\}} \frac{k!(p-k-1)!}{p!} (f(S \cup \{j\}) - f(S)),$$

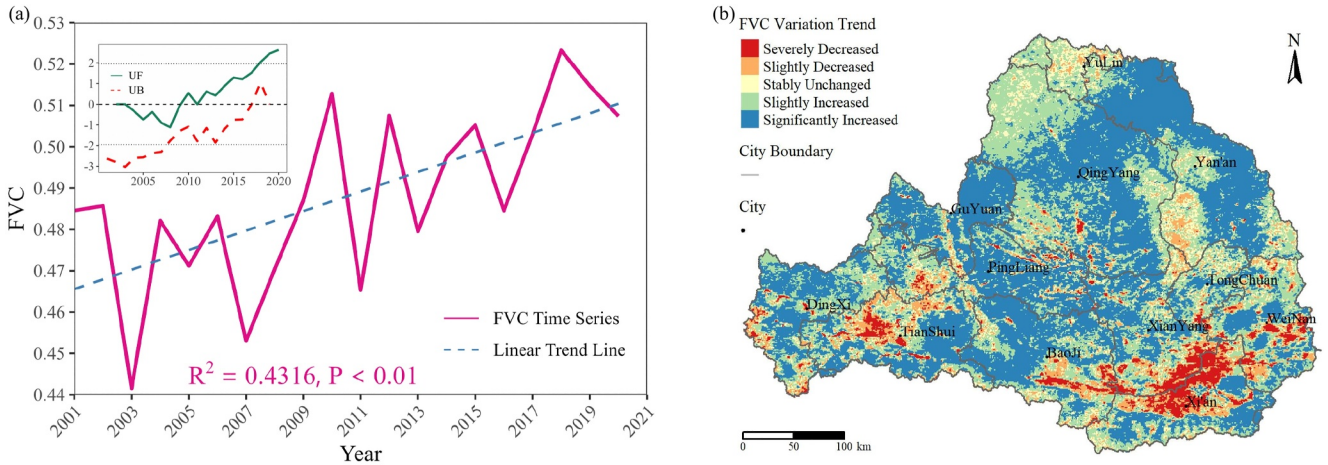

Figure 3. Temporal variation trend (a) and spatial change trend (b) of vegetation coverage in the Weihe River Basin from 2001 to 2020.

where p is the total number of features; $N\backslash\{j\}$ is all subsets of features excluding X_j; S is any subset of features from $N\backslash\{j\}$; k is the remaining number of features in N after removing S; $f(S)$ represents the model prediction with the features in set S; and $f(S \cup \{j\})$ represents the model prediction with the features in set S combined with X_j (Li et al., 2008).

2.3.4. Structural Equation Modeling

Structural Equation Modeling (SEM) is a statistical analysis method that integrates relationships between latent variables and observed variables, relationships between independent and dependent variables, as well as the mediating effects between them, so as to comprehensively analyze the relationships among multiple variables (Doncaster, 2007). The goodness-of-fit of the model can be evaluated using various statistical indicators, such as the Comparative fit index (CFI), Goodness of fit index (GFI), Incremental fit index (IFI), Root mean square error of approximation (RMSEA) and Standardized root mean square residual (SRMR).

We found that the Structural Equation Modeling was not suitable for the case of large sample size. Thus, spatially balanced sampling was utilized by using the Generalized Random Tessellation Stratified (GRTS) algorithm to reduce the sample size from 59949 to 600 while ensuring the representativeness of samples (Stevens & Olsen, 2004).

3. Results

3.1. Spatiotemporal Change Trends in Vegetation Coverage in the Weihe River Basin

This study utilized Theil-Sen median trend analysis combined with the Mann-Kendall test to examine the spatiotemporal variation characteristics of vegetation coverage in the Weihe River Basin. Additionally, seqMK was employed to identify abrupt changes in annual mean vegetation cover change. According to seqMK, an intersection of UF and UB lines indicates a sudden change in trend within the study time series (Gerstengarbe & Werner, 1999). Figure 3a illustrates the interannual variation trend of vegetation coverage from 2001 to 2020, with the UF and UB values graph shown in the top left corner. The Z value from the Mann-Kendall trend test was 2.628, and the P value was 0.008589 (<0.01), which rejects the null hypothesis of no trend in the time series. Furthermore, our UF and UB curves did not intersect, indicating a consistently increasing trend of vegetation cover change. Overall, vegetation coverage exhibited an upward trend from 2001 to 2020, with a linear increase rate of 2.4% per decade.

We effectively analyzed the vegetation trends in the study area using the Theil-Sen median estimator and the Mann-Kendall test, classifying the results based on the actual circumstances of the S_{EVI} (R. Cao et al., 2014; Yuan et al., 2013). Specifically, areas with S_{EVI} less than −0.0005 were defined as vegetation degradation areas, those with S_{EVI} between −0.0005 and 0.0005 were classified as stable vegetation growth areas, and areas with S_{EVI} greater than or equal to 0.0005 were identified as vegetation improvement areas. Furthermore, at a confidence

Table 2
Trend of the EVI in the Weihe River Basin

S_{EVI}	Z	EVI trend
≥0.0005	≥1.96	Severely Increased
≥0.0005	−1.96–1.96	Slightly Increased
−0.0005–0.0005	−1.96–1.96	Stably Unchanged
<−0.0005	−1.96–1.96	Slightly Decreased
<−0.0005	<−1.96	Significantly Decreased

level of 0.05, the results of the significance test from the Mann-Kendall test were further categorized into significant variation areas ($|Z| \geq 1.96$) and non-significant variation areas ($|Z| < 1.96$). The outcomes of these classifications are presented in Table 2.

Based on the aforementioned classification criteria, we conducted an analysis of the overall vegetation coverage in the Weihe River Basin. The result showed that the overall state of vegetation coverage in the study area has improved (Figure 3b), with improved areas covering the majority of the basin, and significantly improved areas accounting for approximately 50% of the basin area. Degraded areas were mainly distributed in the western and southern parts of the basin, concentrated near the Weihe River channel, and severely degraded areas were primarily located in the vicinity of prefecture-level cities. Among them, the proportions of five vegetation cover gradients, severely decreased, slightly decreased, stably unchanged, slightly increased, and significantly increased areas were 4.57%, 8.73%, 9.10%, 31.06%, and 46.54%, respectively.

3.2. Response of Vegetation Coverage to Climate Change and Human Activities in the Whole Weihe River Basin

To systematically investigate the independent contributions of various driving factors influencing vegetation coverage in the Weihe River Basin and their interactive effects, we utilized XGBoost to quantitatively assess and interpret the feature importance of the machine learning training results, complemented by Shapley values. Furthermore, characteristic action curves of each factor were employed to elucidate the specific response trends of vegetation cover changes to the numerical changes of each driving factor. And distinct driving potentials of the factors on vegetation cover changes were defined herein as the range of each factor's impact intensity on vegetation cover changes in this paper. Greater driving potential corresponds to a larger intensity range, manifested as a steeper distribution SHAP curve.

Figure 4 depicts the rankings of independent (variable self-interaction) contribution order (Figure 4a) and the independent SHAP value curve of each driving factor (Figures 4b–4m). Figure 4a demonstrates the profound impact of NtlC, Elev, PreSumC, Slope, PreMaxC, and PdC on vegetation cover changes and these influences exhibited a decreasing trend in magnitude. Within a specific range, high values of NtlC, Elev, and PreSumC manifested inhibitory effects on vegetation cover changes. Notably, the inhibitory impact of high values of these factors exceeded the promoting effect of low values. The elevated TmpAvgC value also mitigated the alteration in vegetation cover, albeit to a lesser extent than the aforementioned factors (Figure 4i). Conversely, high values of Slope, and PreMaxC exhibited a promotive effect on vegetation cover changes. Among these factors, NtlC exerted the most significant impact, exhibited a relatively steep distribution curve, a larger SHAP value range and consequently a greater driving potential, while the SHAP value corresponding to Aspect exhibited minimal

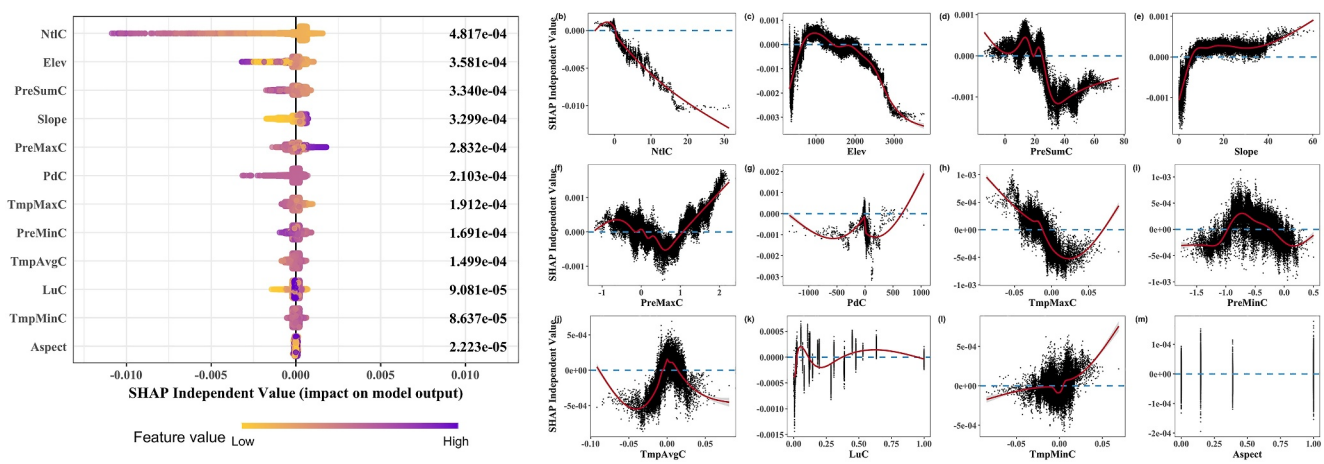

Figure 4. Independent effect of driving factors on vegetation cover change.

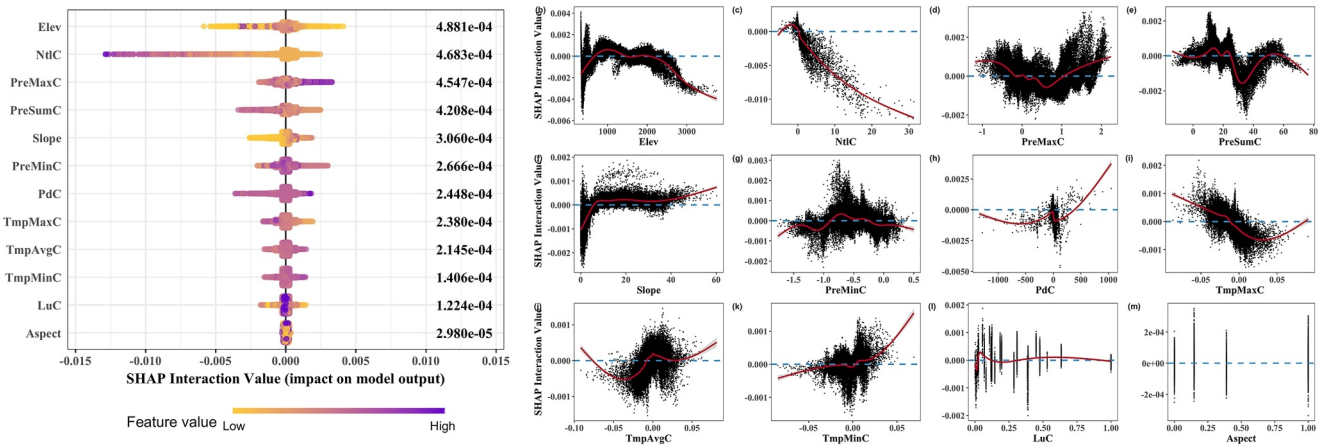

Figure 5. Interactive effect of driving factors on vegetation cover change.

changes, resulting in an almost zero driving potential for independent effects. Other factors, such as Slope, TmpAvgC, LuC, and TmpMinC, had intermediate driving potentials.

Figure 5a delineates the contribution ranking of a specific feature interacting with other features to the model output. The contributions were observed to decrease in the order of Elev, NtlC, PreMaxC, PreSumC, Slope, PreMinC, PdC, TmpMaxC, TmpAvgC, PreMinC, and LuC. Under interaction, Elev exceeded NtlC, which contributed the most under independent action, becoming the variable with the greatest contribution. In Figures 5b–5m, the sample points are vertically spaced apart. This indicated that the interaction of other variables with a specific variable amplified its driving potential, diminished its sensitivity to numerical changes, and expanded the buffer interval for changes in the action direction for vegetation coverage. Within a defined range, the interaction of PreSumC with other variables led to a minimum SHAP value. Consequently, it transitioned from a reduction of the negative effect following independent action to a positive effect within a specific interval post-negative effect reduction. Eventually, it manifested as an increasing negative effect from zero. Similarly, the interaction of TmpAvgC with other variables resulted in a maximum SHAP value. This interaction caused a shift from a reduction in a positive effect after independent action to an increase in a negative effect, followed by a transition to a reduced positive effect and subsequently an increased positive effect.

Aspect remained to have an insignificant effect on the model output after interacting. Elev (0.36%/10a independently and 0.49%/10a interactively) and NtLC (0.48%/10a independently and 0.47%/10a interactively) were the top two features in terms of their influence on the model output. Note that the transition range from positive to negative impact values for NtlC on vegetation cover was narrow, both independent and interactive. This implied a heightened sensitivity of vegetation cover changes to NtlC, and once the threshold of the value was exceeded, restoring a positive impact becomes difficult.

It was indicated that the contribution levels of all factors greatly increased (from 16.38% to 62.73%) after the interaction, with the exception of those of NtlC and Slope, which decreased by 2.77% and 7.24%, respectively (Figure 6). More specifically, under a natural state (factor interaction), most influencing factors exhibited a greater impact on vegetation cover changes compared to the isolated influence of individual factors. The observed reduction in the contribution levels after NtlC interaction may be linked to the mitigation of negative impacts on human activities caused by global climate change. NtlC's interaction with human activities and the self-recovery capacity of ecosystems should also be considered.

3.3. Response to Climate Change and Human Activities in Vegetation Cover Gradients Within the Weihe River Basin

This study employed a structural equation model (SEM) to comprehensively explore the spatial variability and gradient effect of vegetation coverage changes in response to both climate change and human activities within the Weihe River Basin. The final fitted SEM for five vegetation cover gradients (Section 3.1) is shown in Figure 7.

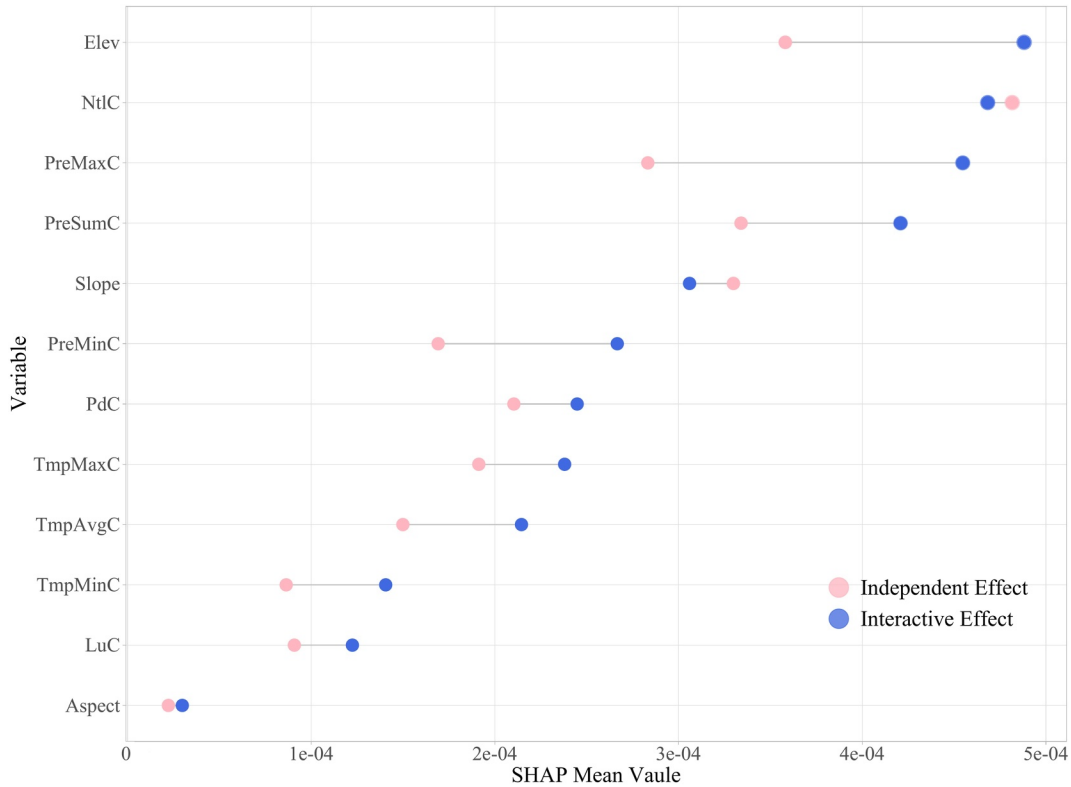

Figure 6. Comparison of the independent and interactive contribution of each factor to vegetation cover change.

The optimization parameters derived from the model fitting for the gradients (Table 3) indicate that the model exhibits a satisfactory fit and meets the required application criteria.

Take the SEM of significantly increased vegetation coverage gradient as an example. The direct and indirect paths of topography, human activity change, and climate change on FVC change based on the SEM are shown in Table 4. By adding up the direct and indirect effects of the latent variables on FVCC, the total effects of topographic, human activity change, and climate change on FVC change were 0.34, 0.20, and −0.74, respectively. In this way, the total effects of topographic, human activity change, and climate change on FVC change of five gradients are shown in Table 5. The analysis of gradient effects is as follows:

(1) Significantly increased vegetation cover gradient

The total effects of topography, human activities, and climate change were 0.34, 0.20, and 0.18, respectively. Topography exerted both direct and indirect effects on FVC changes. Specifically, topography indirectly influenced FVC changes by affecting climate change and human activity change. Notably, among the topographic elements, elevation did not exhibit any discernible effect on FVC changes. This was mainly due to the flat terrain of significantly increased gradient areas. Similarly, among the elements of human activity change, land-use change did not impact FVC changes, indicating a relatively limited variation in land use within this gradient.

(2) Slightly increased vegetation cover gradient

In contrast to the significantly increased gradient areas, topographic elements did not exert a direct impact on FVC changes in areas with slightly increased vegetation coverage. Moreover, SEM identified land-use change to influence human activities, demonstrating a high load factor compared with the other four gradients. This underscored the pronounced role of land-use change in this specific gradient. Overall, the total effects of topography, human activities, and climate change on FVC changes were determined as −0.05, 0.24, and 0.07, respectively.

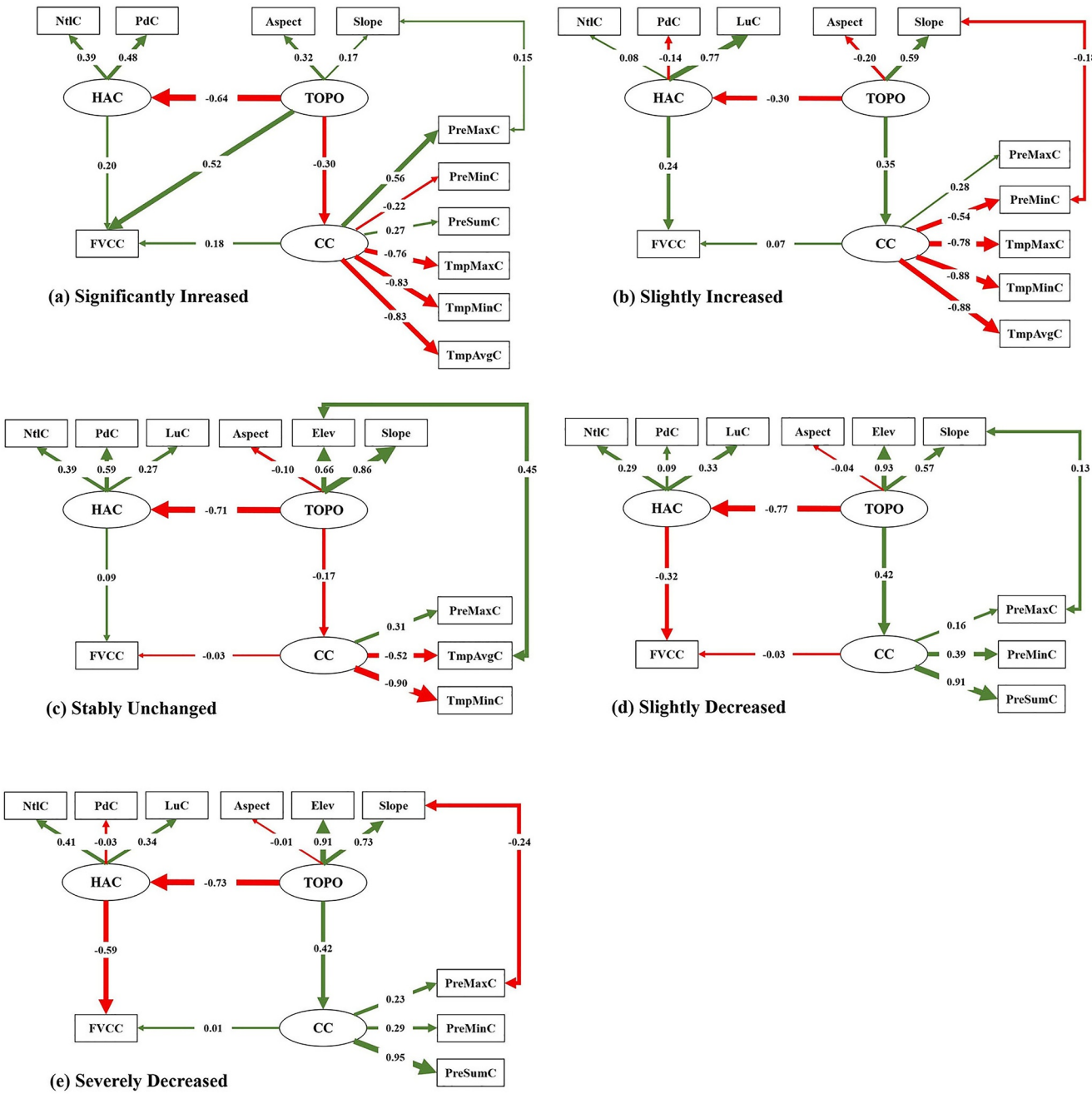

Figure 7. The fitted SEMs for significantly increased, slightly increased, stably unchanged, slightly decreased and severely decreased vegetation coverage gradients.

Table 3
Fitting Effect of the SEM for Vegetation Cover Change Gradients

Fitting optimization index	Adaptation standard	Significantly increased	Slightly increased	Stably unchanged	Slightly decreased	Severely decreased
CFI	>0.90	0.99	0.94	0.94	0.96	0.95
GFI	>0.90	0.95	0.93	0.93	0.94	0.93
IFI	>0.90	0.99	0.94	0.94	0.97	0.95
RMSEA	<0.08	0.02	0.06	0.06	0.03	0.06
SRMR	<0.05	0.03	0.04	0.04	0.03	0.04

Table 4
The Direct, Indirect and Total Effects Among Topographic (TOPO), Human Activity Change (HAC), Climate Change (CC) and FVC Change (FVCC) Based on the Statistically Significant SEM Paths Are Observed in the Significantly Increased Vegetation Coverage Gradient

Impact	Paths	Effect
Direct	TOPO→HAC	−0.64
	TOPO→CC	−0.30
	TOPO→FVCC	0.52
	HAC→FVCC	0.20
	CC→FVCC	0.18
Indirect	TOPO→HAC→FVCC	−0.13
	TOPO→CC→FVCC	−0.05
Total	TOPO→FVCC	0.34
	HAC→FVCC	0.20
	CC→FVCC	0.18

(3) Stably unchanged vegetation coverage gradient

In this gradient, SEM identified elevation to have an impact on topographic elements, indicating considerable fluctuations in elevation within stably unchanged areas. Furthermore, among the observed variables related to climate change elements, only PreMaxC, TmpAvgC, and TmpMinC had an impact on climate change elements. Overall, the total effects of topography, human activities, and climate change were determined as −0.05, 0.09, and −0.03, respectively. Note that there existed a significant correlation between annual mean temperature change and elevation.

(4) Slightly and severely decreased vegetation coverage gradients

In both gradient areas, SEM identified a strong negative impact of human activities on FVC changes, highlighting the pivotal role of human activities in driving FVC changes. Notably, the negative impact of human activities was more pronounced compared to the one in slightly decreased vegetation cover gradient areas. Furthermore, among the observed variables of climate change elements, only precipitation was significant, implying that precipitation is the key climatic factor influencing vegetation coverage changes in the two gradients. This was due to the different changing patterns of climate in gradients with increased, unchanged, and decreased vegetation coverage. In slightly decreased gradient areas, precipitation primarily exerts a direct negative impact on FVC changes. This indicates that the adverse impact of water and soil erosion from precipitation contributes to the vegetation coverage decrease in this gradient.

4. Discussion

4.1. Analysis of the Driving Forces and Gradient Effects of Vegetation Cover Change

The overall vegetation coverage in the Weihe River Basin exhibited an upward trend from 2001 to 2020, which was consistent with previous studies on the Northwest region and the Loess Plateau (Dai et al., 2011; Fu et al., 2011). The contribution of precipitation to vegetation coverage changes found in this study was stronger than that of temperature and elevation, and the results of the changes in the interaction mechanism between factors

Table 5
Response Characteristics of Vegetation Cover Changes in Five Vegetation Cover Gradients

Driver	Significantly increased	Slightly increased	Stably unchanged	Slightly decreased	Severely decreased
Topographic	0.34	−0.05	−0.05	0.23	0.43
Climate change	0.18	0.07	−0.03	−0.03	0.01
Human activities	0.20	0.24	0.09	−0.32	−0.59

were also reflected in other regions of China (Lin et al., 2022; Sun et al., 2020; Wang et al., 2022). Moreover, SEMs were established on the five vegetation cover change gradients divided by Sen slope and MK trend test, revealing terrain and human activity changes as the dominant influencing factors on vegetation cover changes. Among them, human activity changes had a positive effect on areas where vegetation coverage improves and stabilizes, and a negative effect on areas where vegetation coverage degrades. This is related to the two-sided nature of human activities. Policies such as protection and afforestation can have a positive impact on vegetation growth and recovery, while excessive logging and urbanization can lead to vegetation degradation, thereby exerting a negative impact on vegetation coverage. The results obtained in this study, including the greater driving potential, numerical sensitivity, and the decrease in the intensity of negative effects of nighttime light brightness changes after interaction with other factors, all indicated the important role of human activities. Remaining vigilant toward the buffer zone threshold when the direction of action shifts, and comprehensively accounting for the potential positive impacts stemming from interactions with other regional factors can address this issue. Identifying the mechanisms underlying the effects of factors on vegetation cover changes across different gradients, coupled with an alert to the intervals of change in the direction of factor effects, may contribute to fostering positive changes in vegetation coverage.

4.2. Response of Vegetation Cover Change to Extreme Climate

Previous research on the driving forces of vegetation cover change typically focused on annual temperature and total annual rainfall variations as indicators of climate change (Gu et al., 2022), overlooking the impact of potential extreme climate. In fact, extreme climate also has a great impact on vegetation cover change (L. Zhao et al., 2018). Consequently, we accounted for this effect during the specific modeling process, introducing variables such as TmpMaxC, TmpMinC, PreMaxC, and PreMinC into the variable selection. The feature interaction contribution ranking diagram generated by the XGBoost model and interpreted using the SHAP values revealed noteworthy insights. More specifically, the average contribution of PreMaxC in the Weihe River Basin surpassed that of PreSumC, while the average contribution of TmpMaxC exceeded that of TmpAvgC. In the feature-independent contribution ranking, although the average independent contribution of PreMaxC exceeded that of PreSumC, the average independent contribution of TmpMaxC remained higher than that of TmpAvgC. Thus, when modeling changes in vegetation cover, it becomes imperative to enhance model interpretability and alleviate estimation bias by accounting for the extreme effects of climatic conditions.

4.3. Impact of Land Use Change on Vegetation Cover Change

Two primary methods are prevalent for the characterization of land use changes in current studies addressing vegetation changes. One approach involves separately establishing and evaluating models for distinct types of land use changes (G. Yang et al., 2009), and the other involves directly assigning values of 1 and 0 to changing and unchanged land use types, respectively (L. Yang et al., 2021). Both methods, however, are associated with limitations. The former requires the establishment of numerous identical models and cannot distinguish and compare the contributions of land use changes with other explanatory variables. Furthermore, the latter method, despite roughly reflecting inherent changes in land use, overlooks the richness of land use change types, potentially impacting the estimated effect of vegetation changes on land use changes.

This study adopts a compromise method that strikes a balance between the drawbacks of the two prevalent approaches, providing a more comprehensive and finely tuned analysis of the relationship between land use changes and vegetation dynamics. More specifically, we utilized one-hot encoding to pre-encode all types of land use changes, while a random forest model was pre-trained jointly with vegetation changes using ten-fold cross-validation, along with other explanatory variables. Based on feature contribution, weights were assigned to each type of land use change and normalized to the 0–1 range, thus fully utilizing the diversity of land use change types. This allows for the effective quantification of the impact of land use on vegetation cover changes.

4.4. Realistic Modeling Strategies

Numerous studies have shown that, in addition to climate change and human activities, topographic factors also significantly influence vegetation cover change (S.-F. Deng et al., 2013; Pang et al., 2017; J. Zhang et al., 2018; Y. Zhang et al., 2018). The use of linear regression slopes to reflect changes in corresponding variables over time has been proven feasible (M. Zhang et al., 2023). Some studies have also demonstrated the importance of considering

both invariant and variable factors (Liu et al., 2018, 2020). To effectively simulate and reflect real-world conditions, we have made the following considerations, which have informed our modeling strategy:

(1) We selected topographic, human activity, and climate change factors as explanatory variables to investigate their effects on vegetation cover change. Over a nearly 20-year time span, topographic changes are negligible, whereas other variables can exhibit considerable variation. If we exclude topographic factors from our modeling, their influence would be embedded in the residuals, potentially affecting the model's accuracy. Therefore, we assumed that topographic factors remained constant between 2001 and 2020 and incorporated them into the model alongside the changes in other variables represented by their slopes. The modeling we arranged can be likened to fixed effects and random effects. This approach allows us to more clearly observe the impact of topographic factors on vegetation cover change. The modeling results indicated that Elev and slope exerted considerable influence on vegetation cover change, both directly and indirectly, whether in isolation or through interactions.
(2) In reality, multiple elements do not function entirely on their own, but interact with other elements. The SHAP values derived from the XGBoost model can effectively separate the independent and interactive effects of features. This is evident in the dumbbell plot that compares independent and interactive effects, where most elements exhibit an increased feature contribution following interaction, while NtlC demonstrates a reduction in average feature contribution compared to its independent contribution after interactions with other elements. This observation may be attributed to the dual nature of human activities, encompassing both positive (e.g., active afforestation and ecological environment protection) and negative (e.g., mine reclamation and high-density urbanization) aspects.
(3) Adapting to local conditions is an important issue that needs to be considered in practical decision-making, so we also explored different vegetation cover gradients separately. The causal relationship network estimated through structural equation modeling across different vegetation change trend gradients underscores the multidirectional and complex nature of vegetation changes on climate change and human activities. This facilitates access to target different gradients of vegetation cover change for mechanistic understanding and management options, offering valuable insights into the multi-faceted impacts within the studied ecosystem.

4.5. Uncertainties in This Study

Although the study effectively utilized the diversity of land use change types, it represented land use changes using the initial and final years within the research time range, neglecting the temporal fluctuation effects of land use changes. This limitation may introduce inaccuracies in estimating the impact of land use changes on vegetation dynamics. Future modeling efforts should incorporate both the diversity and temporal fluctuation characteristics of land use type changes. In addition, further feature engineering for land use types is recommended to enhance the precision in assessing their impact on vegetation.

Note that in the application of the structural equation model for vegetation changes in this study, the samples were obtained through spatial balanced sampling with the GRTS algorithm. However, spatial effects, such as spatial spillover effects of vegetation change responses to climate change and human activities, were not directly considered in the modeling process. Future modeling endeavors should account for spatial impacts, and the use of spatially explicit structural equation models is recommended to achieve a more accurate estimation of vegetation change responses to climate change and human activities in a spatial context. This approach can contribute to a more comprehensive understanding of the complex interplay between spatial factors and vegetation dynamics.

5. Conclusions

This study employed various methods such as the Sen slope and MK trend tests to explore the impact and contribution of driving factors including climate change, human activities, and topographic elements on vegetation cover changes in the Weihe River Basin, as well as the spatial effects of their changing gradients. Based on the results, we determined the following conclusions:

(1) From 2001 to 2020, the vegetation cover in the Weihe River Basin exhibited an overall improving trend. Elev and NtlC emerged as significant influencers of vegetation cover, with high values of these driving factors exerting a negative impact on its improvement within a specific range. Notably, precipitation demonstrated a greater influence on vegetation cover changes compared to temperature. Furthermore, the adverse effects of extreme climatic conditions on vegetation cover cannot be ignored.

(2) Interplay between climate change and human activities altered the strength of drivers influencing vegetation cover changes. After factor interactions, the driving potential increased and the numerical sensitivity decreased. With the exception of NtlC and Slope, the impacts of other factors were enhanced after factor interactions. Notably, total annual precipitation changes briefly produced a positive effect in high-value areas.
(3) Climate change, human activities, and topographical elements exhibited different directions of action across different vegetation cover gradients. The gradient was divided into five classes by Sen slope and MK trend test to reveal key patterns. Topographical elements exhibited negative effects on the slightly increased and stably unchanged gradients of vegetation cover, whereas positive effects were observed in the remaining gradients. In contrast, climate change elements showed negative effects on the stably unchanged and slightly decreased gradients, but positive effects on the other gradients. Similarly, the human activity elements exerted negative effects on the slightly decreased and severely decreased gradients, with positive effects on the other gradients. Therefore, the topographical and human activity elements are the dominant factors influencing vegetation changes in the Wei River Basin, while the role of climate change is relatively small but cannot be disregarded.

In summary, this study explored the complex and multi-directional response mechanisms of vegetation cover to climate change, human activities, and topographic factors, as well as their interactions. The influence mechanism of vegetation cover change was discussed from the perspective of spatial heterogeneity. The outcomes of this research can be used to evaluate the achievements of sustainable development in China, enrich existing research, and offer a valuable reference for addressing global climate change.

Data Availability Statement

The topographical factor data utilized in this study can be accessed at https://developers.google.com/earth-engine/datasets/catalog/USGS_SRTMGL1_003#bands. Temperature and precipitation data can be downloaded from https://cstr.cn/18406.11.Meteoro.tpdc.270961, https://doi.org/10.11888/Meteoro.tpdc.270961, and https://doi.org/10.5281/zenodo.3114194. Population data is available at https://hub.worldpop.org/doi/10.5258/SOTON/WP00675. Night time light data can be accessed at https://doi.org/10.3974/geodb.2022.06.01.V1. Land use data and the fraction of vegetation cover data are available at https://developers.google.com/earth-engine/datasets/catalog/MODIS_061_MCD12Q1#bands and https://developers.google.com/earth-engine/datasets/catalog/MODIS_MOD09GA_006_EVI#bands respectively.

Acknowledgments
This work was performed with financial support from Natural Science Basic Research Plan of Shaanxi Province (2023-JC-YB-275), in part by National Natural Science Foundation of China (42071144, 42330501), in part by National College Students Innovation and Entrepreneurship Training Program (202310718041).

References

Cao, J., Chi, D., Wu, L., Liu, L., Li, S., & Yu, M. (2008). Mann-Kendall examination and application in the analysis of precipitation trend. *Agricultural Science & Technology and Equipment*, (5), 35–37. https://doi.org/10.3969/j.issn.1674-1161.2008.05.013

Cao, R., Jiang, W., Yuan, L., Wang, W., Lv, Z., & Chen, Z. (2014). Inter-annual variations in vegetation and their response to climatic factors in the upper catchments of the Yellow River from 2000 to 2010. *Journal of Geographical Sciences*, *24*(6), 963–979. https://doi.org/10.1007/s11442-014-1131-1

Chen, C., Zhu, L., Tian, L., & Li, X. (2019). Spatial-temporal changes in vegetation characteristics and climate in the Qinling-Daba Mountains. *Acta Ecologica Sinica*, *39*(9), 3257–3266. https://doi.org/10.5846/stxb201801300252

Chen, T., He, T., Benesty, M., Khotilovich, V., Tang, Y., Cho, H., et al. (2015). Xgboost: Extreme gradient boosting. *R Package Version 0.4-2*, *1*(4), 1–4. https://CRAN.R-project.org/package=xgboost

Dai, S., Zhang, B., Wang, H., Wang, Y., Guo, L., Wang, X., & Li, D. (2011). Vegetation cover change and the driving factors over northwest China. *Journal of Arid Land*, *3*(1), 25–33. https://doi.org/10.3724/sp.J.1227.2011.00025

Deng, C., Bai, H., Gao, S., Liu, R., Ma, X., Huang, X., & Meng, Q. (2018). Spatial-temporal variation of the vegetation coverage in Qinling Mountains and its dual response to climate change and human activities. *Journal of Natural Resources*, *33*, 425–438. https://doi.org/10.11849/zrzyxb.20170139

Deng, S.-F., Yang, T.-B., Zeng, B., Zhu, X.-F., & Xu, H.-J. (2013). Vegetation cover variation in the Qilian Mountains and its response to climate change in 2000–2011. *Journal of Mountain Science*, *10*(6), 1050–1062. https://doi.org/10.1007/s11629-013-2558-z

Ding, Y. X., & Peng, S. Z. (2020). Spatiotemporal trends and attribution of drought across China from 1901–2100. *Sustainability*, *12*(2), 477. https://doi.org/10.3390/su12020477

Doncaster, C. P. (2007). *Structural equation modeling and natural systems*. Wiley Online Library. https://doi.org/10.1111/j.1467-2979.2007.00260.x

Ebrahimi Khusfi, Z., & Zarei, M. (2020). Relationships between meteorological drought and vegetation degradation using satellite and climatic data in a semi-arid environment in Markazi Province, Iran. *Journal of Rangeland Science*, *10*(2), 204–216. https://rangeland.borujerd.iau.ir/article_669564.html

Fang, Z., Bai, Y., Jiang, B., Alatalo, J. M., Liu, G., & Wang, H. (2020). Quantifying variations in ecosystem services in altitude-associated vegetation types in a tropical region of China. *Science of the Total Environment*, *726*, 138565. https://doi.org/10.1016/j.scitotenv.2020.138565

Farr, T. G., Rosen, P. A., Caro, E., Crippen, R., Duren, R., Hensley, S., et al. (2007). The Shuttle Radar Topography Mission. *Reviews of Geophysics*, *45*(2). https://doi.org/10.1029/2005rg000183

Feng, D., Yang, C., Fu, M., Wang, J., Zhang, M., Sun, Y., & Bao, W. (2020). Do anthropogenic factors affect the improvement of vegetation cover in resource-based region? *Journal of Cleaner Production*, *271*, 122705. https://doi.org/10.1016/j.jclepro.2020.122705

Friedl, M., & Sulla-Menashe, D. (2022). MODIS/Terra+Aqua Land Cover Type Yearly L3 Global 500m SIN Grid V061 [Dataset]. *NASA EOSDIS Land Processes Distributed Active Archive Center*. https://doi.org/10.5067/MODIS/MCD12Q1.061

Friedman, J. H. (2001). Greedy function approximation: A gradient boosting machine. *Annals of Statistics*, *29*(5), 1189–1232. https://doi.org/10.1214/aos/1013203451

Fu, B., Liu, Y., Lv, Y., He, C., Zeng, Y., & Wu, B. (2011). Assessing the soil erosion control service of ecosystems change in the Loess Plateau of China. *Ecological Complexity*, *8*(4), 284–293. https://doi.org/10.1016/j.ecocom.2011.07.003

Gerstengarbe, F.-W., & Werner, P. C. (1999). Estimation of the beginning and end of recurrent events within a climate regime. *Climate Research*, *11*(2), 97–107. https://doi.org/10.3354/cr011097

Gu, Z., Zhang, Z., Yang, J., & Wang, L. (2022). Quantifying the influences of driving factors on vegetation EVI changes using structural equation model: A case study in Anhui province, China. *Remote Sensing*, *14*(17), 4203. https://doi.org/10.3390/rs14174203

Huo, H., & Sun, C. (2021). Spatiotemporal variation and influencing factors of vegetation dynamics based on Geodetector: A case study of the northwestern Yunnan Plateau, China. *Ecological Indicators*, *130*, 108005. https://doi.org/10.1016/j.ecolind.2021.108005

Jiang, L., Bao, A., Guo, H., & Ndayisaba, F. (2017). Vegetation dynamics and responses to climate change and human activities in Central Asia. *Science of the Total Environment*, *599*, 967–980. https://doi.org/10.1016/j.scitotenv.2017.05.012

Jiang, M., He, Y., Song, C., Pan, Y., Qiu, T., & Tian, S. (2021). Disaggregating climatic and anthropogenic influences on vegetation changes in Beijing-Tianjin-Hebei region of China. *Science of the Total Environment*, *786*, 147574. https://doi.org/10.1016/j.scitotenv.2021.147574

Kendall, M. G. (1949). Rand correlation methods. https://doi.org/10.2307/1402637

Kumar, A., Jhariya, M., Yadav, D., & Banerjee, A. (2017). Vegetation dynamics in Bishrampur collieries of northern Chhattisgarh, India: Eco-restoration and management perspectives. *Environmental Monitoring and Assessment*, *189*(8), 1–29. https://doi.org/10.1007/s10661-017-6086-0

Kumar, V., Bharti, B., Singh, H. P., & Topno, A. R. (2023). Assessing the interrelation between NDVI and climate dependent variables by using granger causality test and vector auto-regressive neural network model. *Physics and Chemistry of the Earth, Parts A/B/C*, *131*, 103428. https://doi.org/10.1016/j.pce.2023.103428

Li, M. Y., Zhang, X., Wu, W., & Xi, Q. (2008). Spatial balanced sampling for forest resources inventory based on GIS. *Forest and Grassland Resources Research*, *0*(4), 137–142. https://doi.org/10.3969/j.issn.1002-6622.2008.04.031

Lin, M., Hou, L., Qi, Z., & Wan, L. (2022). Impacts of climate change and human activities on vegetation NDVI in China's Mu Us Sandy Land during 2000–2019. *Ecological Indicators*, *142*, 109164. https://doi.org/10.1016/j.ecolind.2022.109164

Liu, Z., Liu, Y., & Li, Y. (2018). Anthropogenic contributions dominate trends of vegetation cover change over the farming-pastoral ecotone of northern China. *Ecological Indicators*, *95*, 370–378. https://doi.org/10.1016/j.ecolind.2018.07.063

Liu, Z., Wang, J., Wang, X., & Wang, Y. (2020). Understanding the impacts of 'Grain for Green'land management practice on land greening dynamics over the Loess Plateau of China. *Land Use Policy*, *99*, 105084. https://doi.org/10.1016/j.landusepol.2020.105084

Ma, Z., Guo, J., Li, W., Cai, Z., & Cao, S. (2021). Regional differences in the factors that affect vegetation cover in China. *Land Degradation & Development*, *32*(5), 1961–1969. https://doi.org/10.1002/ldr.3847

Mann, H. B. (1945). Nonparametric tests against trend. *Econometrica: Journal of the Econometric Society*, *13*(3), 245–259. https://doi.org/10.2307/1907187

Naeem, S., Zhang, Y., Tian, J., Qamer, F. M., Latif, A., & Paul, P. K. (2020). Quantifying the impacts of anthropogenic activities and climate variations on vegetation productivity changes in China from 1985 to 2015. *Remote Sensing*, *12*(7), 1113. https://doi.org/10.3390/rs12071113

Nan, L., Yang, M., & He, S. (2021). Analysis of spatial and temporal distribution characteristics of precipitation in Chongqing from 1965 to 2014. *Yangtze River*, *52*(S2), 64–69. https://doi.org/10.16232/j.cnki.1001-4179.2021.S2.015

Nie, T., Jiang, X., Deng, C., Cai, W., Lei, Y., & Gao, S. (2024). Analysis of the evolution of water culture and water security in the Weihe River Basin over a 100 year-period. *Science of the Total Environment*, *920*, 171066. https://doi.org/10.1016/j.scitotenv.2024.171066

Pang, J., Shangguan, Z., & Wang, G. (2017). The influence of topographic factors on vegetation activity in arid and semi-arid regions of China. *Science of the Total Environment*, *598*, 203–213. https://doi.org/10.1016/j.scitotenv.2017.04.076

Peng, S., Ding, Y., Liu, W., & Li, Z. (2019). 1 km monthly temperature and precipitation dataset for China from 1901 to 2017. *Earth System Science Data*, *11*(4), 1931–1946. https://doi.org/10.5194/essd-11-1931-2019

Piao, S.-L., & Fang, J.-Y. (2001). Dynamic vegetation cover change over the last 18 years in China. *Quaternary Sciences*, *21*(4), 294–302. http://www.dsjyj.com.cn/article/id/dsjyj_9377

Piao, S.-L., Wang, X.-H., Park, T., Chen, C., Lian, X., He, Y., et al. (2020). Characteristics, drivers and feedbacks of global greening. *Nature Reviews Earth & Environment*, *1*(1), 14–27. https://doi.org/10.1038/s43017-019-0001-x

Piao, S.-L., Zhang, X.-P., Chen, A.-P., Liu, Q., Lian, X., Wang, X.-H., et al. (2019). The impacts of climate extremes on the terrestrial carbon cycle: A review. *Science China Earth Sciences*, *62*(10), 1551–1563. https://doi.org/10.1007/s11430-018-9363-5

Piao, S.-L., Fang, J.-Y., & Guo, Q.-H. (2001). Application of CASA model to the estimation of Chinese terrestrial net primary productivity. *Chinese Journal of Plant Ecology*, *25*(5), 603. https://www.plant-ecology.com/EN/Y2001/V25/I5/603

Qu, S.-L., Wang, L., Lin, A., Zhu, H., & Yuan, M. (2018). What drives the vegetation restoration in Yangtze River basin, China: Climate change or anthropogenic factors? *Ecological Indicators*, *90*, 438–450. https://doi.org/10.1016/j.ecolind.2018.03.029

Remy, C. C., Lavoie, M., Girardin, M. P., Hély, C., Bergeron, Y., Grondin, P., et al. (2017). Wildfire size alters long-term vegetation trajectories in boreal forests of eastern North America. *Journal of Biogeography*, *44*(6), 1268–1279. https://doi.org/10.1111/jbi.12921

Shapley, L. S. (1953). 17. A value for n-person games. In K. Harold William, & T. Albert William (Eds.), *Contributions to the theory of games (AM-28)* (Vol. II, pp. 307–318). Princeton University Press. https://doi.org/10.1515/9781400881970-018

Shi, S., Yu, J., Wang, F., Wang, P., Zhang, Y., & Jin, K. (2021). Quantitative contributions of climate change and human activities to vegetation changes over multiple time scales on the Loess Plateau. *Science of the Total Environment*, *755*, 142419. https://doi.org/10.1016/j.scitotenv.2020.142419

Stevens, D. L., Jr., & Olsen, A. R. (2004). Spatially balanced sampling of natural resources. *Journal of the American Statistical Association*, *99*(465), 262–278. https://doi.org/10.1198/016214504000000250

Sun, Y.-L., Shan, M., Pei, X.-R., Zhang, X.-K., & Yang, Y.-L. (2020). Assessment of the impacts of climate change and human activities on vegetation cover change in the Haihe River basin, China. *Physics and Chemistry of the Earth, Parts A/B/C*, *115*, 102834. https://doi.org/10.1016/j.pce.2019.102834

Vermote, E., & Wolfe, R. (2015). MYD09GA MODIS/Aqua Surface Reflectance Daily L2G Global 1kmand 500m SIN Grid V006 [Dataset]. *NASA EOSDIS Land Processes Distributed Active Archive Center*. https://doi.org/10.5067/MODIS/MYD09GA.006

Wang, S., Ping, C., Wang, N., Wen, J., Zhang, K., Yuan, K., & Yang, J. (2022). Quantitatively determine the dominant driving factors of the spatial-temporal changes of vegetation-impacts of global change and human activity. *Open Geosciences*, *14*(1), 568–589. https://doi.org/10.1515/geo-2022-0374

WorldPop, & Bondarenko, M. (2020). Individual Countries 1km UN Adjusted Population Density (2000–2020) [Dataset]. *University of Southampton*. https://doi.org/10.5258/SOTON/WP00675

Wu, J., Zhou, Y., Wang, H., Wang, X., & Wang, J. (2023). Assessing the causal effects of climate change on vegetation dynamics in northeast China using convergence cross-mapping. *IEEE Access*, *11*, 115367–115379. https://doi.org/10.1109/ACCESS.2023.3325485

Xie, N. (2021). *The dual response of the change of vegetation coverage on Shaanxi Province to climate change and human activity. (Master)*. Chang'an University. https://doi.org/10.26976/d.cnki.gchau.2021.001058

Yang, G., Bao, A., Chen, X., Liu, H., Huang, Y., & Dai, S. (2009). Study of the vegetation cover change and its driving factors over Xinjiang during 1998–2007. *Journal of Glaciology and Geocryology*, *3*, 436–445. https://doi.org/10.7522/j.issn.1000-0240.2009.0060

Yang, L., Shen, F., Zhang, L., Cai, Y., Yi, F., & Zhou, C. (2021). Quantifying influences of natural and anthropogenic factors on vegetation changes using structural equation modeling: A case study in Jiangsu Province, China. *Journal of Cleaner Production*, *280*, 124330. https://doi.org/10.1016/j.jclepro.2020.124330

Yuan, L., Jiang, W., Shen, W., Liu, Y., Wang, W., Tao, L., et al. (2013). The spatio-temporal variations of vegetation cover in the Yellow River Basin from 2000 to 2010. *Acta Ecologica Sinica*, *33*(24), 7798–7806. https://doi.org/10.5846/stxb201305281212

Zhang, C., Li, J., Zhou, Z., & Sun, Y. (2021). Application of ecosystem service flows model in water security assessment: A case study in Weihe River Basin, China. *Ecological Indicators*, *120*, 106974. https://doi.org/10.1016/j.ecolind.2020.106974

Zhang, J., Zhang, Y., Qin, S., Wu, B., Wu, X., Zhu, Y., et al. (2018). Effects of seasonal variability of climatic factors on vegetation coverage across drylands in northern China. *Land Degradation & Development*, *29*(6), 1782–1791. https://doi.org/10.1002/ldr.2985

Zhang, M., Wang, K., Liu, H., Yue, Y., Ren, Y., Chen, Y., et al. (2023). Vegetation inter-annual variation responses to climate variation in different geomorphic zones of the Yangtze River Basin, China. *Ecological Indicators*, *152*, 110357. https://doi.org/10.1016/j.ecolind.2023.110357

Zhang, X., Wang, K., Yue, Y., Tong, X., Liao, C., Zhang, M., & Jiang, Y. (2017). Factors impacting on vegetation dynamics and spatial non-stationary relationships in karst regions of southwest China. *Acta Ecologica Sinica*, *37*(12), 4008–4018. https://doi.org/10.5846/stxb201611192354

Zhang, Y., Gao, J., Liu, L., Wang, Z., Ding, M., & Yang, X. (2013). NDVI-based vegetation changes and their responses to climate change from 1982 to 2011: A case study in the Koshi River Basin in the middle Himalayas. *Global and Planetary Change*, *108*, 139–148. https://doi.org/10.1016/j.gloplacha.2013.06.012

Zhang, Y., Shen, Z., & Li, Y. (2018). Impacts of topography on vegetation dynamics in mountainous regions of China. *Ecological Indicators*, *93*, 189–197. https://doi.org/10.1016/j.ecolind.2018.05.006

Zhao, L., Dai, A., & Dong, B. (2018). Changes in global vegetation activity and its driving factors during 1982–2013. *Agricultural and Forest Meteorology*, *249*, 198–209. https://doi.org/10.1016/j.agrformet.2017.11.013

Zhao, W., Li, J., Chu, L., Wang, T., Li, Z., & Cai, C. (2019). Analysis of spatial and temporal variations in vegetation index and its driving force in Hubei Province in the last 10 years. *Acta Ecologica Sinica*, *39*(20), 7722–7736. https://doi.org/10.5846/stxb201809011864

Zhong, X., Yan, Q., Li, G., & Li, G. (2022). Long time series nighttime light dataset of China (2000-2020) [Dataset]. *Digital Journal of Global Change Data Repository*, *6*(3), 416–424. https://doi.org/10.3974/geodb.2022.06.01.V1

Zhou, W., Gang, C., Li, J., Zhang, C., Mu, S., & Sun, Z. (2014). Spatial-temporal dynamics of grassland coverage and its response to climate change in China during 1982–2010. *Acta Geographica Sinica*, *69*(1), 15–30. https://doi.org/10.11821/dlxb201401002

Zhu, C., Peng, W., Zhang, L., Luo, Y., Dong, Y., & Wang, M. (2019). Study of temporal and spatial variation and driving force of fractional vegetation cover in upper reaches of Minjiang River from 2006 to 2016. *Acta Ecologica Sinica*, *39*(5), 1583–1594. https://doi.org/10.5846/stxb201805040993

Zhu, L., Sun, S., Li, Y., Liu, X., & Hu, K. (2023). Effects of climate change and anthropogenic activity on the vegetation greening in the Liaohe River Basin of northeastern China. *Ecological Indicators*, *148*, 110105. https://doi.org/10.1016/j.ecolind.2023.110105